Journal of Power Sources 269 (2014) 1–6

Contents lists available at ScienceDirect

Journal of Power Sources

journal homepage: www.elsevier.com/locate/jpowsour

High durability and hydroxide ion conducting pore-filled anion exchange membranes for alkaline fuel cell applications

Yun Zhao [a, b], Hongmei Yu [a, *], Feng Xie [a], Yanxi Liu [a], Zhigang Shao [a], Baolian Yi [a]

[a] Laboratory of Fuel Cells, Dalian Institute of Chemical Physics, Chinese Academy of Sciences, 457 Zhongshan Road, Dalian, Liaoning 116023, PR China
[b] Graduate School of the Chinese Academy of Sciences, Beijing 100039, PR China

HIGHLIGHTS

- The pore-filled anion exchange membranes are successfully prepared.
- The membranes exhibit high ionic conductivity and excellent alkaline durability.
- The fuel cell with the resulting membranes shows excellent high power out.

GRAPHICAL ABSTRACT

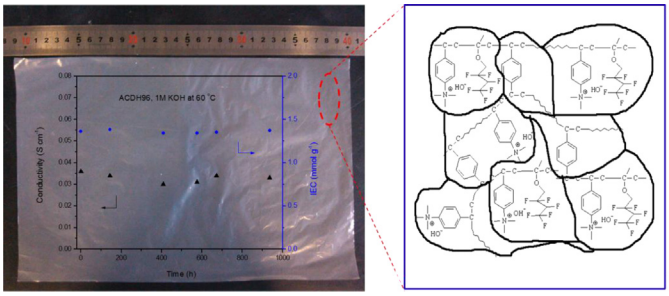

ARTICLE INFO

Article history:
Received 30 November 2013
Received in revised form
3 June 2014
Accepted 4 June 2014
Available online 12 June 2014

Keywords:
Alkaline anion exchange membrane
Ionic conductivity
Polymer electrolytes
Fuel cells
Polyethylene

ABSTRACT

A series of composite anion exchange membranes are successfully synthesized by thermal polymerization of chloromethyl monomer in a porous polyethylene (PE) substrate followed by amination with trimethylamine for alkaline anion exchange membrane fuel cells (AAEMFCs) application. These membranes exhibit excellent alkaline durability and high ionic conductivity. The resulting alkaline anion exchange membranes (AAEMs) show a hydroxide conductivity up to 0.057 S cm^{-1} at 30 °C in deionized water and do not exhibit significant changes in the ionic conductivity and the IEC in 1 M KOH solution at 60 °C for around 1000 h. The maximum power density of 370 mW cm^{-2} is obtained at 50 °C for H_2/O_2 AAEMFC.

1. Introduction

There have been great demands for clean energy or renewable energy sources in the past decade. Fuel cells have attracted considerable attention due to their high energy efficiency and low pollution level. For the fuel cells operated in low temperatures, typically below 100 °C, there are basically two types of fuel cells distinguished by the different ions being transported in the electrolyte, proton exchange membrane fuel cells (PEMFCs) and AAEMFCs. In the past decades, most of the attention was focused on PEMFC due to the invention of the commercial Nafion which possesses a suitable combination of high ionic conductivity and excellent chemical stability [1,2]. Despite of the great success, there are still many challenging barriers which hinder their way of popularization and are difficult to overcome. Among the limitations, the dependence on noble metal catalyst is the critical one. AAEMFCs have begun to attract a lot of attention recently because of the significant advantages of AAEMFCs over PEMFCs in terms of

* Corresponding author. Tel.: +86 411 84379051; fax: +86 411 84379185.
E-mail address: hmyu@dicp.ac.cn (H. Yu).

http://dx.doi.org/10.1016/j.jpowsour.2014.06.026
0378-7753/

high kinetic for oxygen reduction and fuel oxidation in alkaline environment, and the lower cost by using non-precious metal catalysts [3].

In an AAEMFC system, AAEM is a key component which is used to conduct anions and prevent gas crossover. Recently, many groups have devoted to producing AAEMs. Polymer such as polysulfone [4], poly (phthalazinon ether sulfone ketone) [5], poly (arylene ether sulfone) [6], poly (ether ketone) [7], poly (ether sulfone) cardo [8], and poly (ether ether ketone) [9] based AAEMs are investigated by successive chloromethylation and quaternization. The properties of AAEMs will have a significant impact on the performance and durability of AAEMFCs. In particular, high performance AAEMs are required to have high ionic conductivity, mechanical strength and dimensional stability simultaneously. To avoid dilemma between ionic conductivity and stability, some methods and techniques have been commonly utilized including chemical crosslinking technique, physical pore-filling and reinforcement techniques. Na's and Zhuang's group reported AAEMs by a simple self-crosslinking strategy respectively, the stability of the membranes are obviously enhanced by crosslinking technique [10,11]. Coates and co-workers reported the synthesis of a series of cross-linked AAEMs through the ring-opening metathesis polymerization of tetraalkylammonium-fuctionalized cyclic olefins [12,13]. Yamaguchi and co-workers prepared anion exchange pore-filing membrane by filling polyelectrolyte [14]. Another enhanced membrane method is reinforcement technique. Porous PTFE membrane has been adopted as supporting material due to its great mechanical strength, thermal and chemical stability, dimensional stability, lower cost and availability of thinner membranes. PTFE membrane reinforcement technique is considered as one of the most effective methods to increase membrane mechanical strength especially in fabricating reinforced proton exchange membranes [15,16]. In our previous study, we reported quaternary ammonia polysulfone/PTFE and crosslinked quaternary ammonia poly (vinybenzyl)/PTFE composite membranes [17,18]. Although the membranes exhibited high ionic conductivity and good dimensional stability, our previous study encountered one problem: the membranes showed poor chemical stability especially in alkaline solution. Some reasons may be explained this problem: (1) quaternary ammonia group decomposition by OH^- attack [19], (2) material compatibility between porous membrane matrix and polymer. Because PTFE membrane is a hydrophobic and high porous material and the anionic exchange polymer is generally aromatic main chain unlike Nafion with C–F main chain, it has poor compatibility between matrix and polymer. So the polymer will be apt to fall apart from PTFE matrix in long-term alkaline solution. Moon's group reported AAEM from 4-vinylbenzyl chloride crosslinked by divinylbenzene via polymerization in PE matrixe followed by quaternization, this membrane showed good stability in alkaline solution [20].

In this work, we first attempted to prepare the pore-filled anion exchange membranes refer to the method reported by Moon [20]. To further improve the performance of the membranes, we inducted another fluoromonomer into the copolymer to construct "hydrophilic–hydrophobic micro-phase separation" structure. The fabricated membranes exhibited high conductivity and excellent durability in alkaline environment.

2. Experimental

2.1. Materials and composite membrane fabrication

Porous polyethylene used as a substrate was provide from Wide (porous PE, thickness: 20 μm and porosity: 40–50%). 4-vinylbenzyl chloride (VBC, Aldrich), 2, 2, 3, 4, 4, 4-hexafluorobutyl methacrylate (HFM, Aldrich), divinylbenzene (DVB, Aldrich), and benzoylperoxide (BPO) were used as monomer, cross-linker, and thermal initiator, respectively.

Two monomer solution were prepared: (a) 96 mol% VBC, 4 mol% DVB and 0.12 mol% BPO, (b) 96(98) mol% VBC, 4(2) mol% DVB, 2 mol% HFM and 0.12 mol% BPO. Then, a porous PE substrate was immersed in the monomer solution for 10 min at room temperature to allow for complete impregnation of monomers into the porous substrate. After the monomer sorption process, the PE substrates were sandwiched between two pieces of glasses, and polymerized at 100 °C for 12 h. After the polymerization, it was aminated by soaking in trimethylamine (TMA) or a mixture of TMA and acetone (3:1 by vol.) for 48 h at room temperature. The quaternized membranes were washed with water. The membrane was subsequently soaked in 1 M KOH for 48 h. Finally, the resulting membranes were washed and stored in deionized water.

2.2. FTIR characterization

ATR-FTIR of membranes was obtained on a JASCO FT-IR 4100 spectrometer with an ATR accessory containing a Ge crystal with a wavenumber resolution of 4 cm^{-1} and range of 500–4000 cm^{-1}.

2.3. Ion exchange capacity, water uptake, swelling behavior and mechanical strength

The ion exchange capacity (IEC) of the membranes was determined by titration method. The membrane with OH^- forms was soaked in 0.01 M HCl solution for 48 h at 30 °C. Subsequently, HCl was titrated against 0.01 M aqueous solution of NaOH with phenolphthalein as indicator. The IEC was calculated as follows

$$\mathrm{IEC} = \frac{M_{\mathrm{o,HCl}} - M_{\mathrm{e,HCl}}}{m} \tag{1}$$

where $M_{\mathrm{o,HCl}}$ and $M_{\mathrm{e,HCl}}$ are moles of HCl before and after titration with NaOH, respectively, and m is the weight of the membrane.

Water uptake was measured by immersing the membrane into water at 30 °C for 24 h. Then the membranes were taken out, wiped with a tissue paper, and quickly weighed on a microbalance. The weights of the dry membranes were obtained after drying at 60 °C under vacuum for 24 h. The water uptake Wu (wt%) could be calculated as follows:

$$\mathrm{Wu(wt\%)} = \frac{W_{\mathrm{wet}} - W_{\mathrm{dry}}}{W_{\mathrm{dry}}} \times 100\% \tag{2}$$

where W_{dry} and W_{wet} are the weights of dry and hydrated membranes, respectively.

The swelling ratio could be calculated as follows

$$\text{Swelling ratio } (\%) = \frac{L_{\mathrm{wet}} - L_{\mathrm{dry}}}{L_{\mathrm{dry}}} \times 100\% \tag{3}$$

The dimension (length, width and thickness) of sample was taken in the OH^- form when it was fully hydrated and dried, respectively. The drying of sample was carried out at 60 °C for 24 h.

The mechanical property of the membranes was measured with a WDW Electromechanical Universal Testing Machine at room temperature. The membrane specimens were of 10 mm width and tested using a programmed elongation rate of 50 mm min^{-1}. Before the measurements, the membrane samples were kept in DI water at room temperature overnight and water on the surface was absorbed with filter paper.

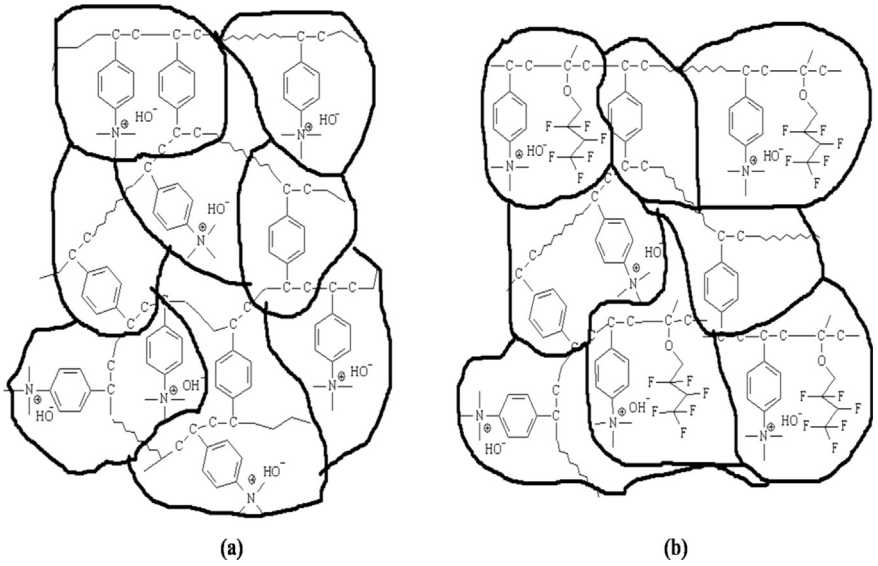

Fig. 1. A schematic of the crosslinked bipolymer and terpolymer composite AAEMs. The bold black lines represent PE chains.

2.4. Ionic conductivity measurement

The ionic conductivity was determined by using a cell with a pair of pressure-attached copper electrodes coating gold. The resistance of the membrane was measured by using electrochemical impedance spectroscopy (EIS) using a Solartron 1260 frequency response analyzer coupled to a Solartron 1287 potentiostat. Signal amplitude of 10 mV in the frequency range of 1 MHz–0.1 Hz was applied. Before the measurement, the membrane was kept in DI water to minimize its exposure to ambient CO_2. The membrane sample was taken out quickly, and then sealed between two plates with electrodes of testing fixture, which was placed in DI water to keep a relative humidity of 100%. Moreover, DI water was updated before every measurement. The membrane conductivity (σ, S cm^{-1}) could be calculated by the following equation

$$\sigma = \frac{L}{RS} \tag{4}$$

where L (cm) is the distance between the working electrode and reference electrode, S (cm^2) is the membrane cross sectional area, and R (Ω) is the membrane resistance, which is obtained by simulating from the AC impedance data (Ω).

2.5. MEA preparation and fuel cell tests

MEA was prepared as follows: A commercial catalyst Pt/C (70%, JM Co.) was mixed with a certain amount of water, isopropyl alcohol and AS-4 ionomer solution (Tokuyama Co.), and then sonicated to obtain a homogenous ink. The Pt loading in the anode and cathode were both 0.4 mg cm^{-2}. The abovementioned catalyst ink was brushed onto a gas diffusion layer (GDL, Toray-060) to form a conventional gas diffusion electrode. MEA was comprised of an AAEM sandwiched between an anode and a cathode, and hot-pressed at 60 °C, 1 MPa for 2 min. Fuel cell test was carried out with H_2 and O_2 at 50 °C with 100% relative humidity (RH). The flow rate of H_2/O_2 was 100/200 ml min^{-1} at 0.05 MPa, respectively.

3. Results and discussion

3.1. General scheme for AAEMs

AAEMs were prepared with two kinds of monomer solution, which structure were is illustrated in Fig. 1. The bold black lines represent the porous PE chains. The structure of the crosslinked quaternized poly (vinybenzyl-divinylbenzene) bipolymer and the crosslinked quaternized poly (vinybenzyl-divinylbenzene-hexafluorobutyl methacrylate) terpolymer were shown in Fig. 1(a) and (b), respectively. The monomer HFM was highly hydrophobic due to the existence of abundant F element, to some extent, it enhanced "hydrophilic-hydrophobic micro-phase separation" of the membranes, which can provide continuous pathways for ion transport.

3.2. FTIR analysis

The FTIR spectra of porous PE substrate and the fabricated membranes were presented in Fig. 2. The intense peaks at 2918 and

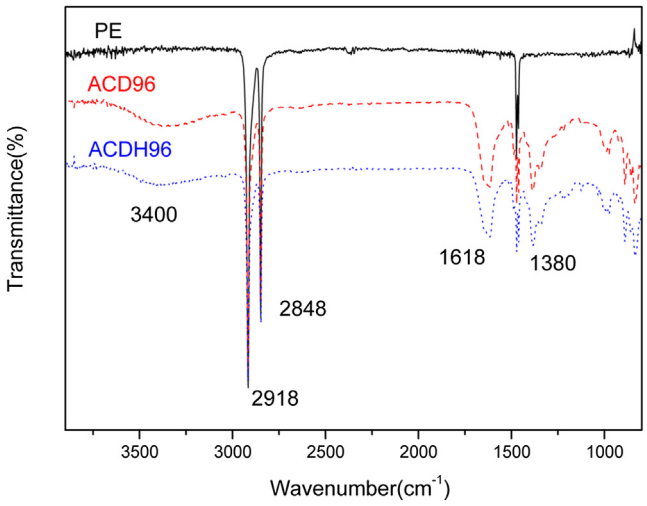

Fig. 2. FT-IR spectra of PE, ACD96 and ACDH96 membranes.

Table 1
Membrane properties of AAEMs.

Membranes	CMS:DVB:HFM	IEC (meq g^{-1})	Water uptake (wt%)	Swelling ratio (%), 30 °C			Conductivity (S cm^{-1}), 30 °C	Thickness (μm), in dry state	Mechanical strength (MPa)
				L	*W*	*T*			
CD96[a]	96:4:0	1.45	43.4	1	2	35	0.022	22	–
ACD96[b]	96:4:0	1.54	59.8	3	3	45	0.03	22	115.1
ACDH96[b]	96:4:2	1.35	42.2	2	3	28	0.035	22	99.7
ACDH98[b]	98:2:2	1.76	65.0	2	2	55	0.057	23	102.3

Reaction conditions for quaternization. a: TMA; b: TMA and acetone.

2848 cm^{-1} for all the samples were attributed to $-CH_3$ and $-CH_2$ stretching vibration from the original PE substrate [20]. After polymerization and quaternization, a new absorption band at 1618 cm^{-1} appeared which corresponds to C=C stretching vibration in an aromatic rings, and a typical C–N vibration peak was observed near 1380 cm^{-1} [21], implying that monomers were successfully copolymerized within the porous PE substrate. The strong band near 3400 cm^{-1} in the ACD96 and ACDH96 spectrum correspond to the quaternary ammonium group stretching vibration [22]. As such, these results show that pore-filled AAEMs were prepared successfully.

3.3. Ion exchange capacity, water uptake, swelling ratio and mechanical strength

The IEC, water uptake and swelling ratio of each AAEM were listed in Table 1. IEC provided an indication for the quaternary ammonium groups present in a polymer matrix, which was responsible for the conduction of anions and provided a reliable approximation of the ionic conductivity. The IEC of the CD96 (1.45 meq g^{-1}) with TMA as the quaternized reagent was lower than that of the ACH96 (1.54 meq g^{-1}) with a mixture of TMA and acetone as the quaternized reagent. This may be because the membrane facilitated swelling in acetone by making the quaternization easier. The IEC of the ACDH96 decreased to 1.35 meq g^{-1} due to increase in the monomer fraction of the copolymer. The maximum IEC (1.74 meq g^{-1}, ACDH98) can be obtained as increasing the VBC content in monomer composition.

The water uptake of the fabricated membranes showed a linear increase from 42.2 to 65.0% as the IEC increased. The swelling ratio of the fabricated membranes were also showed in Table 1. All the membranes exhibited good dimensional stability in the length and width direction because of the restriction effect of the PE substrate. However, the swelling ratio of the membranes in the thickness direction were obviously larger than that in the length and width direction at room temperature. This may be because the anionic polymer on the surface of the PE substrate exhibited highly swelling in the vertical plane. The dimensional stability of the ACDH96 was better than that of the ACD96 and CD96 due to low water uptake as inducting the monomer HFM.

The mechanical properties of the fabricated membrane were measured at room temperature and 100% RH. As shown in Table 1, the mechanical strengths of ACD96, ACDH96 and ACDH98 were 115.1, 99.7 and 102.3 MPa, respectively. The composite membranes display excellent mechanical property due to the reinforcement of porous PE substrate.

3.4. Ionic conductivity

The hydroxide ionic conductivity of the membrane is a key parameter, which is closely related to fuel cell performance. As is shown in Table 1, the conductivities of the CD96, ACD96, ACDH96 and ACDH98 at 30 °C were 0.022, 0.03, 0.035 and 0.057 S cm^{-1}, respectively. The trend of the conductivity accorded with that of the IEC. Fig. 3 showed the temperature dependent ionic conductivities of the ACD96, ACDH96, ACDH98 along with Nafion 211 (measured under identical conditions; Nafion has been frequently used as a benchmark for conductivity assessment of various membranes including AAEM [13]). All conductivities increased with the testing temperature. The ACDH98 with low crosslinked degree exhibited an anionic conductivity of 0.057 S cm^{-1} at 30 °C. This conductivity is high compared with that of most of AAEMs such as radiation-grafted ETFE AAEM (around 0.03 S cm^{-1} at 50 °C) [23], cross-linked composite AAEM (0.032 S cm^{-1} at 25 °C) [18], and SCL-TPQPOH (0.038 S cm^{-1} at 20 °C) [24].

3.5. Thermal stability

The thermal stability of the prepared membranes as well as pristine PE substrate were investigated in a nitrogen atmosphere at a heating rate of 10 °C min^{-1} (Fig. 4). Before the measurement, the dry membrane samples were placed on the balance to absorb water until the weight reached the equilibrium at room temperature. The original porous PE substrate displayed a single step degradation, whereas the resulting composite membrane exhibited three step degradation processes. It attracts water from the atmosphere due to the strong hydrophilicity of the quaternary ammonium group, a weight loss below 100 °C corresponding to the evaporation of absorbed water was observed. This behavior has been commonly found in other polymeric ion exchange membranes. The second step of weight loss was around 140–200 °C, related with quaternary ammonium groups decomposition [22]. The final step between 400 and 500 °C was the decomposition of polyethylene backbone. It could also be obtained from Fig. 4 that the amount of infiltrated copolymer is around 30 wt% of the total composite membrane weight.

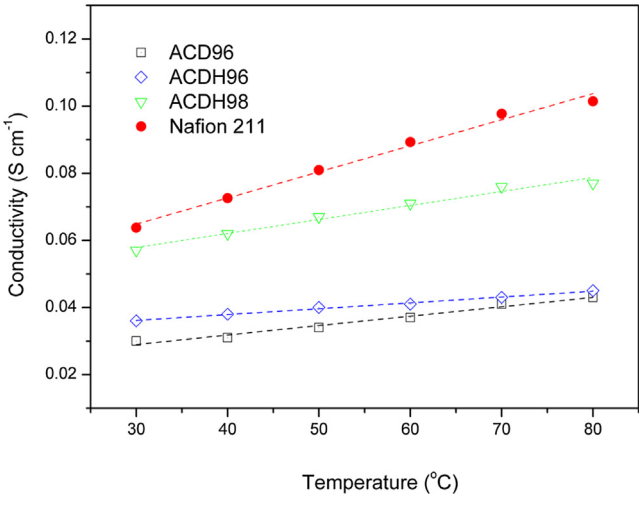

Fig. 3. Temperature dependence of ionic conductivities of the membranes.

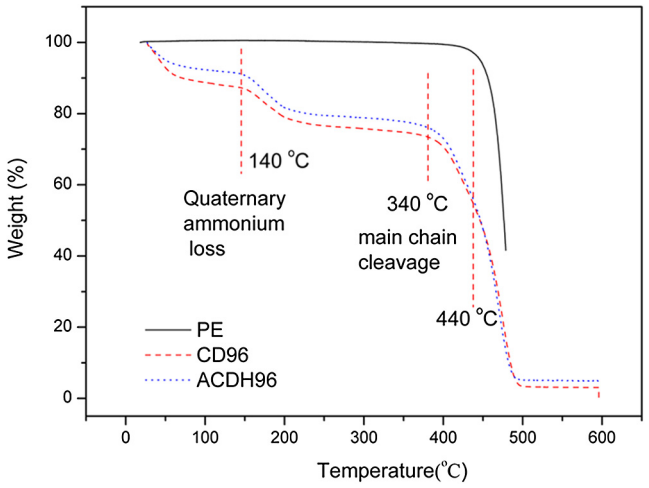

Fig. 4. TGA of PE, CD96 and ACDH96 membranes.

3.6. Chemical stability

To meet the requirements of the practical application in fuel cells, besides the excellent thermal stability and high ionic conductivity, the prepared AAEMs must have good chemical stability, especially in the high pH environment of alkaline fuel cells. However, to the best of our knowledge, there was few reports on the stability of the AAEMs in long-term alkaline solution. PEK based AAEM prepared by Chen showed alkaline stability in 1 M KOH solution at 60 °C for 120 h [25]. Bis-imidazolium based AAEM prepared by Yan exhibited good long-term stability in 1 M KOH solution at 60 °C for 30 days [26]. Here, the chemical stability of the CD96 and ACDH96 was evaluated by immersing them in 1 M KOH under 60 °C. The stability of the membranes in alkaline condition was then assessed based on the change of the ionic conductivity and IEC during the test period (Fig. 5). During the test, it was found that the ionic conductivities and IEC values of the CD96 and ACDH96 did not significantly change even after exposure upto about 1000 h, indicating that the fabricated composite pore-filled AAEMs were relatively stable in 1 M KOH solution.

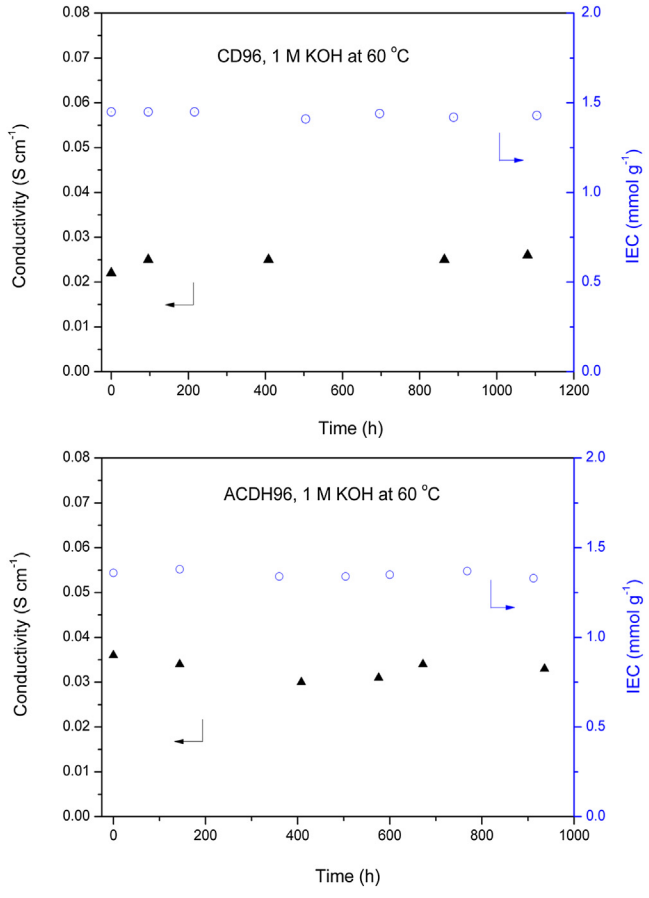

Fig. 5. Alkaline stability of CD96 and ACDH96 membranes in 1 M KOH solution at 60 °C.

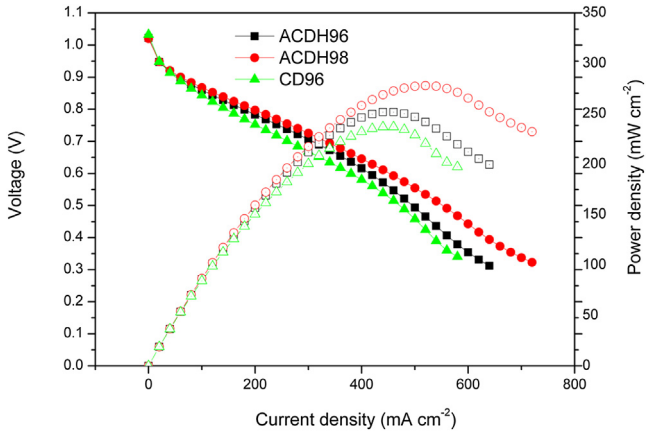

Fig. 6. *I–V* polarization curves of the fuel cells with the ACD96, ACDH96 and ACDH98 membranes.

3.7. Fuel cell performance

The polarization performances of AAEMFCs with the different membranes were shown in Fig. 6. As shown in Fig. 6, the open circuit voltages (OCVs) reached over 1.02 V with the fabricated membranes in the fuel cell tests, which is in the range of typical alkaline fuel cell. This result indicated that the fabricated membranes had no significant gas crossover. The performance of the ACDH98 with a maximum power density of 278 mW cm^{-2} was better than that of the ACDH96 (252 mW cm^{-2}) and CD96 (237 mW cm^{-2}) due to its high conductivity. To obtain a higher cell performance, we tried to adjust the proportion of the electrode. The

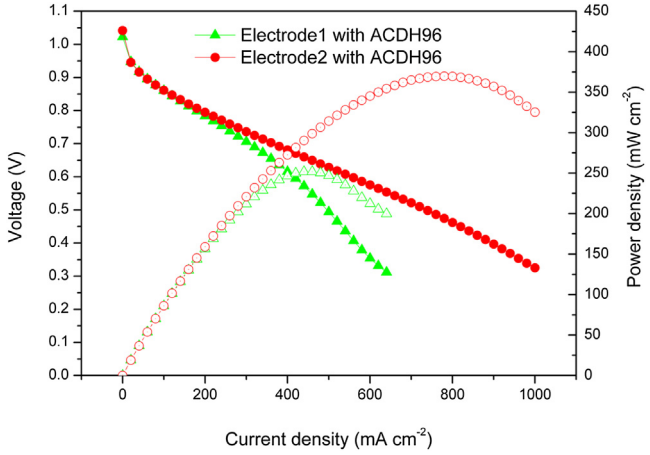

Fig. 7. The cell performance of the different electrode with the ACDH96 membrane.

Table 2
The peak power density of H_2–O_2 AEMFC reported.

AEMs	Thickness [μm]	P_{max} [mW cm^{-2}]	Cell temperature [°C] (back pressure, [kPa])	Pt loading [mgPt cm^{-2}]	Ionomer
ACDH96 (this work)	22	370	50 (0.05)	0.4	AS-4
QAPS/PTFE [17]	20	315	50 (0.05)	0.4	AS-4
TPPVBN30 [18]	26	338	60 (0.05)	0.4	AS-4
TPQPOH152 [27]	50	258	70 (0.25)	0.2	TPQPOH124
Radiation-grafted AEM [28]	80 (wet)	210	50 (0)	0.5	t-PVBTMACl
FAA [29]	70	200	80 (0.25)	0.5	TPQAOH
QPMBV-APE [30]	50	180	70 (0.1)	0.4	QPMBV
qPVB/OH^- [31]	50	156	15 (0)	0.8	qPVB/OH^-
PTFE-QDPSU [32]	30 (wet)	146	50 (0)	0.5	QDPSU

ACDH96 was used as the electrolyte due to its low water uptake and swelling ratio. The best performance of the electrode2 with the ACDH96 was shown with a maximum power density of 370 mW cm^{-2} in Fig. 7. It could be attribute to the optimization of the electrode structure. This is compared with the performance ever reported for AAEMFC (Table 2).

4. Conclusions

The pore-filled anion exchange membranes were prepared for AAEMFC application. The fabricated membranes exhibited excellent alkalline stability after exposure upto about 1000 h in 1 M KOH solution. The AAEMFC with the resulting membrane showed a high cell performance. These results suggest that the fabricated pore-filled anion exchange membranes in this work are promising in AAEMFCs application.

Acknowledgments

This work was financially supported by the National High Technology Research and Development Program of China (863 Program, No. 2011AA050705), National Basic Research Program of China (973 Program, No. 2012CB215500) and the National Natural Science Foundation of China (No. 21176234, No. 20876154).

References

[1] J. Choi, K.M. Lee, R. Wycisk, P.N. Pintauro, P.T. Mather, J. Mater. Chem. 20 (2010) 6282–6290.
[2] B. Dong, L. Gwee, C. Salas-de la, K.I. Winey, A. Elabd, Nano Let. 10 (2010) 3785–3790.
[3] G.F. Mclean, T. Niet, S. Prince-Richard, N. Djilali, Int. J. Hydrogen Energy 27 (2002) 507–526.
[4] J. Pan, S.F. Lu, Y. Li, A.B. Huang, L. Zhuang, J.T. Lu, Adv. Funct. Mater. 20 (2010) 312–319.
[5] J. Fang, P.K. Shen, J. Membr. Sci. 285 (2006) 317–322.
[6] Y. Xiong, Q.L. Liu, Q.H. Zeng, J. Power Sources 193 (2009) 541–546.
[7] G.G. Wang, Y.M. Weng, J. Zhao, R.R. Chen, D. Xie, J. Appl. Polym. Sci. 112 (2009) 721–727.
[8] L. Wu, T.W. Xu, D. Wu, X. Zheng, J. Membr. Sci. 310 (2008) 577–585.
[9] X.M. Yan, G.H. He, S. Gu, X.M. Wu, L.G. Du, H.Y. Zhang, J. Membr. Sci. 375 (2011) 204–211.
[10] J. Ni, C.J. Zhao, G. Zhang, Y. Zhang, J. Wang, W.J. Ma, Z.G. Liu, H. Na, Chem. Commun. 47 (2011) 8943–8945.
[11] J. Pan, Y. Li, L. Zhuang, J.T. Lu, Chem. Commun. 46 (2010) 8597–8599.
[12] T.J. Clark, N.J. Robertson, H.A. Kostalik IV, E.B. Lobkovsky, P.F. Mutolo, G.W. Coates, J. Am. Chem. Soc. 131 (2009) 12888–12889.
[13] N.J. Robertson, H.A. Kostalik IV, T.J. Clark, P.F. Mutolo, H.D. Abruna, G.W. Coates, J. Am. Chem. Soc. 132 (2010) 3400–3404.
[14] H. Jung, K. Fujii, T. Tamaki, H. Ohashi, T. Ito, T. Yamaguchi, J. Membr. Sci. 373 (2011) 107–111.
[15] F.Q. Liu, B.L. Yi, D.M. Xing, J.R. Yu, H.M. Zhang, J. Membr. Sci. 212 (2003) 213–223.
[16] H.L. Tang, M. Pan, F. Wang, P.K. Shen, S.P. Jiang, J. Phys. Chem. B 111 (2007) 8684–8690.
[17] Y. Zhao, J. Pan, H.M. Yu, D.L. Yang, J. Li, L. Zhuang, Z.G. Shao, B.L. Yi, Int. J. Hydrogen Energy 38 (2013) 1983–1987.
[18] Y. Zhao, H.M. Yu, D.L. Yang, J. Li, Z.G. Shao, B.L. Yi, J. Power Sources 221 (2013) 247–251.
[19] C.S. Macomber, J.M. Boncella, B.S. Pivovar, J.A. Rau, J. Therm. Anal. Calorim. 93 (2008) 225–229.
[20] S. Maurya, S.H. Shin, M.K. Kim, S.H. Yun, S.H. Moon, J. Membr. Sci. 443 (2013) 28–35.
[21] F.X. Zhang, H.M. Zhang, J.X. Ren, C. Qu, J. Mater. Chem. 20 (2010) 8139–8146.
[22] S. Singh, A. Jasti, M. Kumar, V.K. Shahi, Polym. Chem. 1 (2010) 1302–1312.
[23] J.R. Varcoe, R.C.T. Slade, E.L.H. Yee, S.D. Poynton, D.J. Driscoll, D.C. Apperley, Chem. Mater. 19 (2007) 2686–2693.
[24] S. Gu, R. Cai, Y.S. Yan, Chem. Commun. 47 (2011) 2856–2858.
[25] H. Zarrin, J. Wu, M. Fowler, Z.W. Chen, J. Membr. Sci. 394-395 (2012) 193–201.
[26] B. Qiu, B. Lin, Z.H. Si, L.H. Qiu, F.Q. Chu, J. Zhao, F. Yan, J. Power Sources 217 (2012) 329–335.
[27] S. Gu, R. Cai, T. Luo, K. Jensen, C. Contreras, Y.S. Yan, ChemSusChem 3 (2010) 555–558.
[28] R. Zeng, J. Handsel, S.D. Poynton, A.J. Roberts, R.C.T. Slade, H. Herman, D.C. Apperley, J.R. Varcoe, Energy Environ. Sci. 4 (2011) 4925–4928.
[29] S. Gu, R. Cai, T. Luo, Z.W. Chen, M.W. Sun, Y. Liu, G.H. He, Y.S. Yan, Angew. Chem. Int. Ed. 48 (2009) 6499–6502.
[30] Y.T. Luo, J.C. Guo, C.S. Wang, D. Chu, ChemSusChem 4 (2011) 1557–1560.
[31] Y.C. Cao, X. Wang, M. Mamlouk, K. Scott, J. Mater. Chem. 21 (2011) 12910–12916.
[32] X. Wang, M.Q. Li, B.T. Golding, M. Sadeghi, Y.C. Cao, E.H. Yu, K. Scott, Int. J. Hydrogen Energy 36 (2011) 10022–10026.